Astronomy & Astrophysics manuscript no. draft
May 3, 2016

Select suitable radio sources to define the celestial frame

N. Liu and J.-C. Liu

School of Astronomy and Space Science, Nanjing University, 210023 Nanjing, PR China
e-mail: liuniu@smail.nju.edu.cn

May 3, 2016

ABSTRACT

Aims. To exclude the sources with unstable behaviors in ICRF2 defining, and add some stable sources to defining a more stable celestial frame.

Methods. A pre-selection is done to select the sources with long and stable observation as the candidates. For these candidate sources, a linear least square fitting is applied to the time series of coordinates of sources, weighed according to the mean error within 3 data spans: 1979.0~1990.0; 1990.0~2009.0; 2009.0~2016.0. Based on the linear drift of $\alpha \cos \delta$ and δ fitted before, sources are ranked in two different ways. Two factors are considered in the source selection scheme: the axial stability and uniform sky distribution.

Results. 4 sets of sources are selected to be suitable for defining a more stable celestial frame, the number of sources being 307, 366, 304 and 324.

Key words. astrometry – reference systems: inteferometric

1. Introduction

In 1994 the International Astronomical Union (IAU) recommended the adoption of a celestial reference system (Arias et al. 1995), realized by the highly precise coordinates of a specific set of extra-galactic radio sources observed at radio wavelength with the Very Long Baseline Interferometry (VLBI), known as the International Celestial Reference System (ICRS) and International Celestial Reference Frame (ICRF). The first realization of the ICRF (hereafter referred to as ICRF1) was proposed by Ma et al. (1998), based on 212 defining sources with a positional accuracy batter than 1 milliarc second (mas) in both coordinate. However, as pointed out by the authors, there are some unknown physical characteristics of radio sources, causing a large drift of coordinates. Several studies on assessing the positional stability for individual sources and the celestial frame axes were undertaken (see Feissel & Gontier 2000; Gontier et al. 2001; Feissel-Vernier 2003; Feissel-Vernier et al. 2006; Gontier & Lambert 2008; Lambert & Gontier 2009). Some ensembles of sources were proposed, showing a better positional time stability for individual sources.

In 2009 an improved version of the ICRF (hereafter referred to as ICRF2) was adopted, including 3414 sources and 295 defining sources therein (Ma et al. 2009; IER 2015). The ICRF2 improves the stability of axes by a factor about 2 compared to the ICRF1 and with more sources in the southern hemisphere selected, therefore has a more uniform sky distribution. But the time stability estimation of the ICRF2 axes, especially in post-ICRF2 observations, should be continued. A recent study (Lambert 2013) shows that there is no noticeable deformation of the ICRF2 axes, but the author suggests that such work should be undertaken regularly as the time series updates. Moreover, the problem in the defining sources selection always exist, which is the relatively poor sky distribution in the southern hemisphere. It has been seven years since the date of the ICRF2 release, what is concerned is whether there are suitable sources to be considered as defining or replace some defining ones. The purpose of this paper is to find that whether there exist the new subsets of sources with improved stability.

Several criteria were adopted in the previous studies. Three aspects of radio sources were mainly investigated in the ICRF1 work(Arias & Bouquillon 2004; Ma et al. 1998), which are: quality of data and observational history; consistency of coordinates derived from subsets of data; repercussions of source structure. Based on these criteria, sources are categorized into three class: defining, candidate, and other. A method to select sources based on the analysis of time series stability of astrometric positions was initially proposed by Feissel-Vernier (2003) and the subset was extended in Feissel-Vernier et al. (2006). A similar selection scheme can be seen in Gontier & Lambert (2008); Lambert & Gontier (2009). Several estimators of time series were investigated in these works, i.e., standard deviation, slope, Allan standard deviation and goodness of fit, while session time series and regular time series(for example, one-year average) show different statistical characteristics. The selection of the ICRF2 defining sources was partly based on the time series (Ma et al. 2009; IER 2015). A stability criterion based on overall positional index and successive structure index defined therein was adopted and accordingly sources were ranked from the most stable to the less. Considering the sky coverage, loose threshold was set for sources in the southern hemisphere.

In this paper, time series of coordinates are investigated to select suitable sources. The principle strategy is to keep the main part of the ICRF2 defining sources and add new stable sources. A pre-selection is done in Sect.2, while a detailed discription of the selection schemes is given in Sect.3. Sect.4 presents some conclusions.

For comparision, some ensembles of sources proposed in the previous studies are used. For clarity, in the following sections, the ICRF1 and ICRF2 defining sources will be referred to as "212 ICRF" and "295 ICRF" respectively, while a subset of 247 sources provided by Feissel-Vernier et al. (2006) will be referred to as "247 MFV".

2. Data and Pre-selection

The Paris Observatory IVS analysis center provides a set of coordinate time series for 3826 sources [1] obtained from VLBI solution (see Lambert 2013, Sect. 2 for details). Fig. 1 presents the observational history of the total 3826 sources, labelled as "3826OPA". It can easily be seen that some non-defining sources have been observed for a long period, more frequently than some defining ones. Previous studies (Lambert & Gontier 2009, for example) usually mentioned that quality of early VLBI data is much worse compared to that of the later, and therefore the data before 1990.0 must be used with much caution. For this reason these studies used the coordinate time series only after 1990.0. In contrast, the authors of the ICRF2 work commented that the positions and corresponding uncertainties generated from the entire available VLBI data can represent realistically how confident to use these positions in the future. For that reason, the full time series from August 1979 up to now are used in this paper.

To exclude sources having a poor observational history or a questionable behavior, a pre-selection algorithm is applied. First, 39 special handling sources with known significant positional instability, 3 known gravitational lenses and 6 known radio stars(see Ma et al. 2009, Sect. 4) are excluded. Then sources are considered as observed well, only when the length of observation span is longer than 10 years and number of sessions sources are observed is larger than 20. This threshold is however artificial and since there is no specific definition of a rich or poor observation history. It should be noticed that for some ICRF2 defining sources, the points of time series become obviously denser after 2009, in which most are located in the southern hemisphere. A too strict threshold will exclude them, which is out of our wish. Finally, 613 sources are kept as candidates, including 291 ICRF2 defining sources. 4 ICRF2 defining sources excluded are: 1448-648, 1554-643, 1611-710, 1633-810. These sources have few points as seen from their time series. The source names used here are the IERS source designations. The observational histories of these sources are shown in Fig. 2. For low declination some non-defining sources are observed several time, and hence may be possibly selected as defining sources.

3. Sources Selection

Although the radio sources are assumed to have no proper motion because of their extremely far distances, the time series of coordinates will show some variability, due to i.e., an immediate rejection of jet or the extend structure, affecting the stability of the celestial frame based on them. The variability can be investigated by statistical estimators, i.e., the goodness of fit considered as an indicator sensitive to random errors. Three estimators are used in this paper: the weighted standard deviation referred to the mean (weighted root mean square), the weighted Allan deviation and the linear drift (slope) of both $\alpha\cos\delta$ and δ coordinates. The standard deviation describes the scatters of the coordinates while the Allan deviation investigates the stochastic properties of coordinates time series, sensitive to abrupt changes of coordinates. And the linear drift estimation is based on an underlying physical assumption, and considered as reliable since time series of these candidates have enough points. In this work, the weighted standard deviation and the weighted Allan deviation are estimated to rule out sources with significantly noisy time series while the normalized linear drift (the ratio of linear drift to its uncertainty) is used as an indicator of positional stability, according to which the sources are ranked from most stable to less in the next precedure.

Annual average points are constructed by taking the weighted mean of all data contained in an one-year interval over 1980.0-2016.0 for determination of the Allan deviation. However, few sources have observational histories dense enough for the Allan deviation test. An extension of the Allan deviation proposed by Malkin (2008) (labelled as "WADEV" in that paper) is used.

Fig. 3 presents the distribution of the weighted standard deviation and the weighted Allan deviation. The result is much larger compared to that of Feissel-Vernier (2003). The possible reason is that the entire time series are used here while post-1990.0 time series were used in that work. Then sources with the weighted standard deviation or the weighted Allan deviation of both coordinates larger than $10mas$ are excluded, and 499 sources are kept.

The linear drifts are obtained using the weighted least squares estimation (denoted by $\mu_\alpha\cos\delta$ and μ_δ respectively), but there is a difference. Consider that the formal error contained in time series may include some model error during the data reduction and not represent the real observational error, average weight over a observational span is used. The time series are divided into three observation spans: 1979.0~1990.0; 1990.0~2009.0; 2009.0~2016.0, on the assumption that each observation span corresponds to different observational accuracies. And the average weight is used as weight of session points within the corresponding observation span. The normal equation of estimation of $\alpha\cos\delta$ coordinate is given by (1) and the one for δ coordinate is similar.

$$\begin{pmatrix} \mu_{\alpha^*} \\ \alpha_0^* \end{pmatrix} = \sum_{i=1}^{3} \begin{pmatrix} \sum_j \frac{(\Delta t_{ij})^2}{\sigma_{ij}^2} & \sum_j \frac{(\Delta t_{ij})}{\sigma_{ij}^2} \\ \sum_j \frac{(\Delta t_{ij})}{\sigma_{ij}^2} & \sum_j \frac{1}{\sigma_{ij}^2} \end{pmatrix}^{-1} \begin{pmatrix} \sum_j \frac{(\Delta t_{ij})\alpha_{ij}^*}{\sigma_{ij}^2} \\ \sum_j \frac{\alpha_{ij}^*}{\sigma_{ij}^2} \end{pmatrix} \tag{1}$$

where $i = 1, 2, 3$ represent the three observation spans respectively, and Δt_{ij} is the difference referred to 2000.0. Similar to the marker used in other papers, $\mu_{\alpha^*} = \mu_\alpha\cos\delta$. Then the linear drift $\mu = \sqrt{\mu_{\alpha^*}^2 + \mu_\delta^2}$.

Fig. 4 shows the linear drift of the three subsets, in which some sources are found to have the linear drift larger than 0.5 mas/yr (marked in red arrows). Although it may be arbitrary to consider sources a large linear drift as unstable, since the corresponding uncertainties of the linear drift may be large too. Actually, a sources with a large linear drift and small corresponding uncertainty is more possible to be unstable (Lambert & Gontier 2009). But a extremely large linear drift is intolerable. For this reason, we keep 549 sources with a large linear drift smaller than 0.5 mas/yr and rank them from the most stable to less according to their normalized linear drift. This rank list will be referred as "Overall Rank list" in the following sections. However, because of the less sources in the southern hemisphere, small number will enter the defining sources list according to Overall Rank list, causing the celestial frame uniform in sky distribution. To loose the threshold for sources with low declination, the ICRF2 work introduces a method in which sources are binned into 6 intervals of declination by four nodes so that each interval has approximately the same number of sources. In each interval, sources are

[1] http://ivsopar.obspm.fr/radiosources/

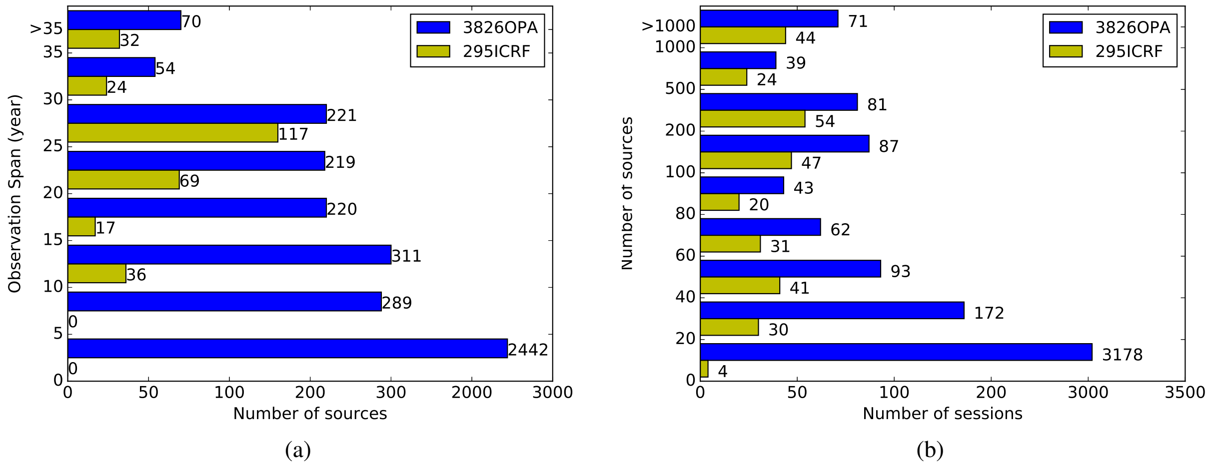

Fig. 1. Statical histograms of length of the observation span (*left*) and amount of the observational session for a individual source (*right*), displaying the observational histories of the 3826 sources.

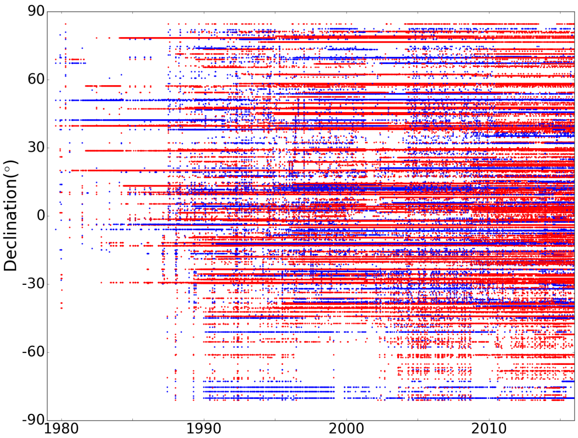

Fig. 2. Observation history of 613 candidates, including 291 ICRF2 defining sources(*red*) and 322 non-defining sources(*blue*).

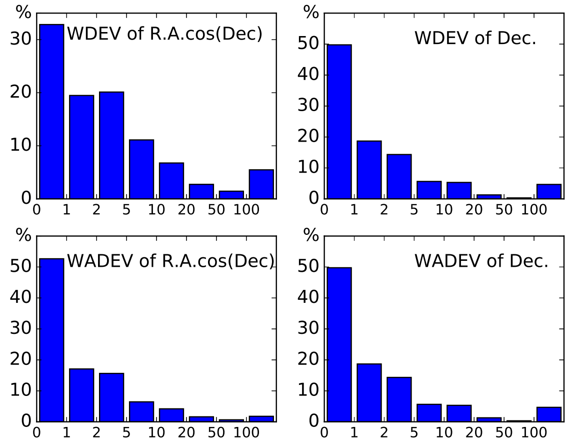

Fig. 3. The statistical histograms of the weighted standard deviation (WDEV) and the weighted Allan deviation (WADEV) for $\alpha\cos\delta$ (*left*) and δ (*right*) coordinates. The units are mas.

given a rank index normalized 100, and ranked. Here a similar way is adopted. The sphere are divided into 4 partitions with the equal spherical area, and the corresponding nodes of the declination are $-30°$, $0°$ and $30°$. The number of sources located in partitions are 101, 127, 168 and 153 respectively. In each partition, similarly, sources are ranked according to the normalized linear drift. In the final rank list, the sources with smaller rank order are ranked more priori, while the ranking priorities of sources with same rank order in different partitions are based on their normalized linear drift. Using this rank strategy, a rank list referred as "Partition Rank list" is established. In the next part, we will determine the subsets of stable sources according these two rank list.

3.1. Considerations on the axial stability

The stability of reference frame axes is usually assessed by using a 4-parameter transformation to model the radio source coordinate difference, which includes three rotation angles and an equatorial tilt. Besides, some other parameters such as slopes in right ascension and declination and three parameters express-

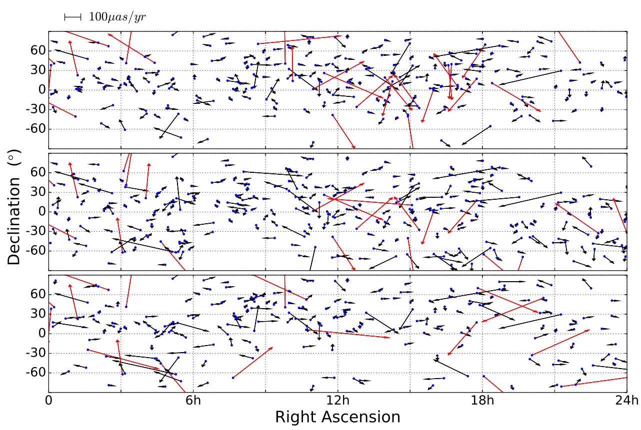

Fig. 4. Linear drift of sources in three subsets: 212 ICRF(*bottom*), 295 ICRF(*middle*) and 247 MFV(*top*). The linear drift larger than 500 $\mu as \cdot yr^{-1}$ is adjusted to 500 $\mu as \cdot yr^{-1}$ and plotted in red arrow.

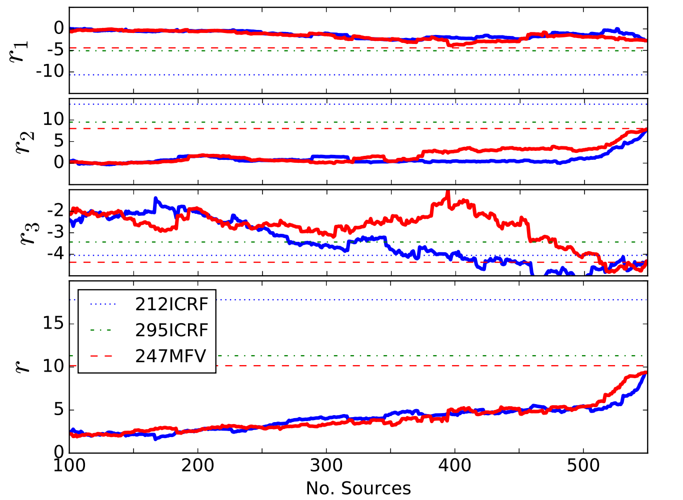

Fig. 5. The fitting results of rotation vector of the Overall Rank (*blue*) and Partition Rank (*red*) list. The three horizontal lines are the results of the three special subsets, as given in the legend.

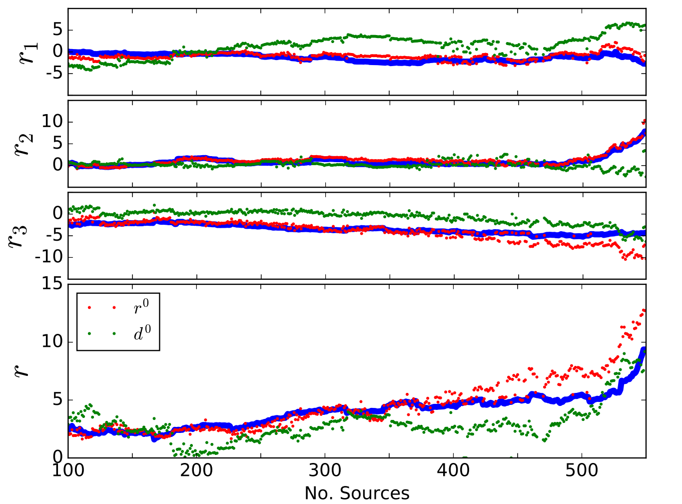

Fig. 6. The fitting results of considering rotation and glide vector both. The blue line is the result shown in Fig . The red and green point are corresponding part of rotation and glide respectively. The rank list is Overall Rank list.

ing a dipolar deformation can be added into the model (see, e.g. Lambert 2013; Mignard & Klioner 2012). Here the one-order spherical harmonics of rotation is used, the corresponding equations are given below.

$$\mu_{\alpha^*}\cos\delta = +r_1\cos\alpha\sin\delta + r_2\sin\alpha\sin\delta - r_3\cos\delta \tag{2}$$

$$\mu_\delta = -r_1\sin\alpha + r_2\cos\alpha, \tag{3}$$

where $\boldsymbol{r} = (r_1, r_2, r_3)^T$is global rotation vector. The difference from the normal way is that we use the average coordinate difference.

Fig. 5 shows that r_1, r_2, r_3 and r evolve with the number of sources. It is obviously seen from the overall trend that as the number increases, more sources with large μ are included in, causing larger axial rotations for both ranks. But there are some eclipses and horns. And for the two rank list, r is approximately equal when the number of sources is below 500, better about a factor of 2 than that for the 295 ICRF.

When using the vector spherical harmonics, the influence of one-order glide vector need to be taken into consideration. The equations are shown in the below:

$$\begin{aligned}\mu_\alpha\cos\delta &= -d_1^0\sin\alpha + d_2^0\cos\alpha \\ &\quad +r_1^0\cos\alpha\sin\delta + r_2^0\sin\alpha\sin\delta - r_3^0\cos\delta \end{aligned}\tag{4}$$

$$\begin{aligned}\mu_\delta &= -d_1^0\cos\alpha\sin\delta - d_2^0\sin\alpha\sin\delta + d_3^0\cos\delta \\ &\quad -r_1^0\sin\alpha + r_2^0\cos\alpha,\end{aligned}\tag{5}$$

where $\boldsymbol{d^0} = (d_1^0, d_2^0, g_3^0)$ is glide vector. A superscript 0 is used to draw a distinction between the rotation vector in different models. Fig. 6 displays the result, which shows that the rotation part is close to the one in Fig. 5, while glide part shows stable referred to some values. For this reason it is reliable to consider rotation vector solely. Higher order vectors are not considered because there is a small number sources to deal with.

3.2. Considerations On the sky distribution

How uniform the sources distribution on the sphere sky is, is another aspect that need to be taken into consideration. The mean declination of subset is one of estimators. (Liu et al. 2012) gives an approach to assess how uniform sources of a subset locate on the celestial sphere., which is to assume a dipolar vector field according the coordinates of sources first and fit it by global rotation (fitting equation similar to 2, denoted by g). The result of that work shows that an ideal uniform ensemble of sources will have a zero rotation. The simulation is used in this work, but the pole of the dipolar vector field is needless to be the Galactic Center, the North pole instead here.

Fig. 7 shows the result of simulation.

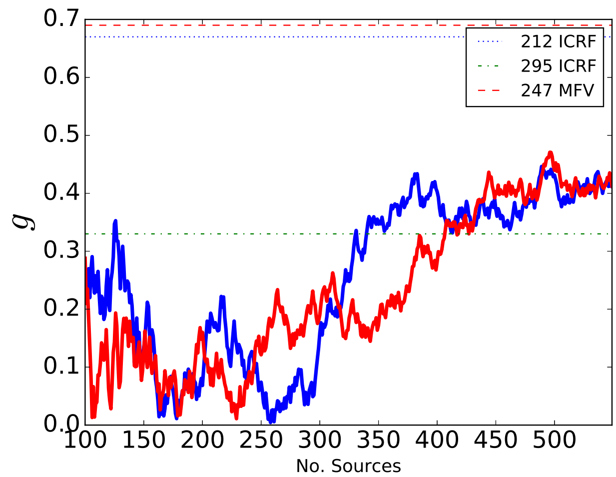

Fig. 7. The results of simulation. The blue and red line are corresponding result of rank1 and rank2 respectively.

3.3. Consideration on above two respects

When considerations on axial ability and sky distribution are taken simultaneously, a quality index of subset is defined as

$$Q = \frac{3 * r_N + g_N}{4}, \tag{6}$$

where r_N and g_N are the results of Fig. 5 and 7 normalized to 1, weighted by 3:1. This weight ratio shows a priori consideration on axial ability. The result of Q is given in Fig. 8 and 4 ensembles of sources with sources among 300-400 are selected (denoted by

Table 1. Mean declination and Source

Source Set	Mean declination	Number of ICRF2 defining
Sou322	-0.13°	140
Sou351	-0.37°	154
Sou371	-0.48°	163
Sou394	-0.51°	173

Notes. The mean declination for 212 ICRF, 295 ICRF2 and 247 MFV are 4.80°, 0.70°, and 16.89° respectively.

Table 2. Axial stability

Source Set	r_1	r_2	r_3	r
Sou322	-1.65±0.29	1.07±0.29	-2.75±0.27	3.39±0.49
Sou351	-2.30±0.26	0.48±0.25	-2.21±0.25	3.22±0.44
Sou371	-2.43±0.24	1.62±0.24	1.62±0.23	3.71±0.41
Sou394	-2.72±0.22	2.37±0.22	-1.00±0.21	3.75±0.38

Notes. The units: $\mu as \cdot yr^{-1}$.

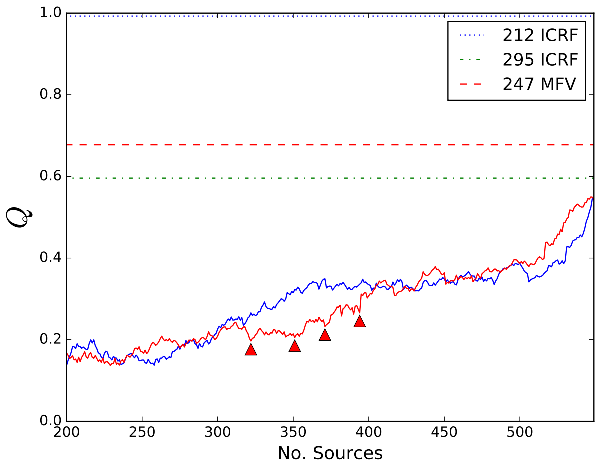

Fig. 8. The Quality index.

Fig. 9. Linear drift of 4 sets of sources to be considered as defining sources. The red points means that the sources is included in 295 ICRF2 defining sources.

red triangles), referred as "Sou322", "Sou351", "Sou371" and "Sou394". The linear drift of sources in these four sets are shown in Fig. 9, most sources showing a tiny linear drift and a good sky coverage. And the corresponding statical information is given in Table. 1, and Table.2.

4. Conclusions

With the time series of coordinates over 30 years for sources, some of ICRF2 defining appear to be unstable and not suitable to defining a celestial frame. 4 sets of sources with improved in both axial stability and uniform sky distribution are recommended.

References

2015, Astron. J., 58, 58
Arias, E. & Bouquillon, S. 2004, Astronomy & Astrophysics, 422, 1105
Arias, E. F., Charlot, P., Feissel, M., & Lestrade, J.-F. 1995, Astron. Astrophys., 303, 604
Feissel, M. & Gontier, A.-M. 2000, in International VLBI Service for Geodesy and Astrometry 2000 General Meeting Proceedings, Vol. 1, 280
Feissel-Vernier, M. 2003, A&A, 403, 105
Feissel-Vernier, M., Ma, C., a. M. Gontier, & Barache, C. 2006, Astron. Astrophys., 452, 1107
Gontier, A.-M. & Lambert, S. 2008, in Journées Systèmes de Référence Spatio-temporels 2007, Vol. 1, 42
Gontier, A.-M., Le Bail, K., Feissel, M., & Eubanks, T. M. 2001, Astron. Astrophys., 375, 661
Lambert, S. 2013, Astronomy & Astrophysics, 553, A122
Lambert, S. B. & Gontier, A.-M. 2009, Astron. Astrophys., 493, 317
Liu, J., Capitaine, N., Lambert, S. B., Malkin, Z., & Zhu, Z. 2012, 50
Ma, C., Arias, E., Eubanks, T., et al. 1998, The Astronomical Journal, 116, 516
Ma, C., Arias, E. F., Bianco, G., et al. 2009, IERS Technical Note, 35
Malkin, Z. 2008, J. Geod., 82, 325
Mignard, F. & Klioner, S. 2012, Astron. Astrophys., 547, A59